PROCEEDINGS, Nineteenth Workshop on Geothermal Reservoir Engineering
Stanford University, Stanford, California, January 18-20, 1994
SGP-TR-147

On the Interpretation of Tracer Experiments

Ibrahim Kocabas
Suleyman Demirel University, Isparta, Turkiye

Roland N. Horne
Stanford University

William E. Brigham
Stanford University

Abstract

Recently, two new developments appeared in the literature on modelling flow and transport in heterogeneous systems. The first one is the use of two different concentration variables namely, the resident and flux concentrations, in tracer studies. The second one involves representing the heterogeneity by means of a frequency disribution function for immobile phase size. Based on these developments, this work involves a classification of the solutions of transport equation in heterogeneous systems. It also demonstrates interpretation of tracer experiments in such systems.

Distinguishing between the resident and flux concentration variables prevents the inconsistencies between theoretical solutions and actual conditions of experiments and hence, allows correct interpretation of tracer return profiles. Representing heterogeneities by means of frequency distribution functions allows representing matrix blocks of various sizes likely to exist in a fractured reservoir.

1 Introduction

Convection-dispersion equation has been the most commonly used model of transport in porous media. Common experience, as summarized by Parker and van Genuchten[1], is that in cases of media with low apparent dispersivities, experiments yielded fairly symmetrical tracer return profiles and solutions of this model matched the observed profiles well. However, in cases of media with large variations in pore water velocities caused by preferential flow paths, experiments yielded asymmetrical tracer return profiles. An apparent cause of this is that some part of pore space could be bypassed resulting in different flux and resident concentrations.

As a result, need arised for re-evaluating the applicability of convection-dispersion model for heterogeneous media. This re-evaluation indicated that some of the limitations come from the failure to distinguish between the resident and the flux concentrations.

Failure to distinguish between these two types of concentrations leads to use of solutions inconsistent with the actual conditions. This point has first been shown by Brigham[2], then Kreft and Zuber[3] classified solutions of convection-dispersion equation in terms of these concentration variables and others followed them.

Modelling flow and transport in heterogeneous media depends on the scale of flow and varies from employing a single fracture located in a porous matrix to considering the entire medium as a single continuum representing the characteristics of both fractures and porous matrix blocks[4].

One of the two recent developments in modelling transport in heterogeneous media is use of frequency distribution functions for the size distribution of matrix blocks [5, 6]. Another development in modelling such systems is representation of the fracture transport equations of the far field approach by a single standard equation by using block geometry functions[7], BGFs.

2 Theoretical Developments

In the following, the above mentioned two new developments are combined to develop solutions to equations of transport in heterogeneous media. The standard equation of transport is nondimensionalized to be made independent of scale. Then, the solutions were classified with regard to the distinction between the resident and flux concentrations.

2.1 Two Concentration Variables in Tracer Studies

A variable of a system is defined as a characteristic which acquires different numerical values at different times. A parameter, on the other hand, is defined as a quantity characterizing the physical processes acting upon the variable and remaining constant in time[8]. In tracer studies, the use of two different variables, namely resident and flux concentrations, has been equally common.

In development of mathematical equations, the resident concentration, C_R, defined as the amount of tracer per unit volume of the system at a given instant, has always been taken as the variable of the system. In experiments, on the other hand, the flux concentration, C_F, defined as the ratio of the tracer flux to the volumetric flux, has been the most commonly measured quantity. As a result, tracer return profiles have been plotted mostly by using the flux concentration as the output variable. These two concentrations differ whenever the system is dispersive and there is a concentration gradient. In a dispersive system the flux and the resident concentration variables are related by:

$$C_F = C_R - \frac{1}{P_e}\frac{\partial C_R}{\partial x_D} \quad (1)$$

where x_D is the dimensionless distance and P_e is the Peclet number. Eq. 1 serves for finding C_F whenever the theoretical form of C_R is known, or vice versa.

Based on C_R, the equation of transport in a one-dimensional linear system is:

$$\mathcal{L}C_R = q_D \quad (2)$$

where q_D is a dimensionless source function, and the linear operator $\mathcal{L}$ is:

$$\mathcal{L} = \frac{1}{P_e}\frac{\partial^2}{\partial x^2_D} - \frac{\partial}{\partial x_D} - \frac{\partial}{\partial t_D} \quad (3)$$

where t_D is the dimensionless time:

$$t_D = \frac{ut}{L} \quad (4)$$

Normally, one would solve Eq.2 for C_R, and then find the expression for C_F by using Eq.1. However, whenever q_D is a linear function of C_R, it is also possible to solve Eq.2 for C_F directly as explained below.

Differentiating Eq.2 with respect to x_D yields:

$$\frac{\partial}{\partial x_D}\mathcal{L}C_R = \frac{\partial q_D}{\partial x_D} \quad (5)$$

Since the solution is required to be continuous in x_D the differentiation can be carried inside the operator:

$$\mathcal{L}\frac{\partial C_R}{\partial x_D} = \frac{\partial q_D}{\partial x_D} \quad (6)$$

Eq.6 states that if the source term q_D is a linear function of C_R, the partial derivative of C_R with respect to x_D is also a solution of Eq.2. Similarly, partial derivatives of any order with respect to either of x_D or t_D yield the same result[9]. In addition, according to the superposition principle, a linear combination of two solutions must also be a solution. Based on this principle, the following particular relation is important:

$$\mathcal{L}\{C_R - \frac{1}{P_e}\frac{\partial C_R}{\partial x_D}\} = q_D - \frac{1}{P_e}\frac{\partial q_D}{\partial x_D} \quad (7)$$

Expressing Eq.7 in terms of C_F:

$$\mathcal{L}C_F = q_F \quad (8)$$

Eq.8 states that when the dependent variable C_R of Eq.2 is transformed to C_F, the form of Eq.2 remains the same. Consequently, it is possible to solve Eq.2 for C_F directly by specifying the initial and boundary conditions properly. Unless a distinction is made between these two concentration variables, material balance errors will occur due to incorrect use of solutions. Such conclusions were also arrived at earlier by several researchers[1, 2, 3] who mostly used the classical convection-dispersion equation and actually performed a dependent variable transformation to show that Eq.2 is also satisfied by C_F. The method employed here, however, is more general and in the following section it will be applied to heterogeneous medium models.

2.2 Modelling Heterogeneous Systems

The classical convection-dispersion equation represents only one of the various approaches in modelling the transport in heterogeneous media. Therefore, it is desirable to generalize classification of solutions to dispersive models by constructing a similar table of solutions for heterogeneous medium models.

A heterogeneous system is characterized by preferential flow paths due to dead end pores, aggregates, fissures, fractures, layering, and so on. Tracer transport in heterogeneous porous media may be modelled in four ways[4] namely, the very near field, the near field, the far field, and he very far field. Names of these various approaches are related to the scale of heterogeneities with respect to the scale of flow.

The very near field is usually conceptualized as a fracture located in a porous matrix. Flow is assumed to occur in the fracture only. The reservoir fluid occupying the pores of the matrix is considered to be virtually immobile. The exchange of tracer between fracture and matrix occurs by molecular diffusion. Tracer concentrations across the fracture are equalized before any significant effect of the convection appears. Within the matrix, diffusive transport is assumed to occur only perpendicular to the flow direction in the fracture.

In the near field, tracer transport in a set of well defined preferential flow paths is considered. When a deterministic approach is chosen the transport equations are identical to equations of the very near field approach.

In the far field approach, tracer transport is modelled by using two superposed continua, a mobile phase composed of a network of preferential flow paths, and an immobile phase representing the rest of the system. Immobile phase is assumed to act as a distributed source in mobile phase. Transfer from mobile to immobile phase may be assumed proportional to the difference between average concentrations of the two phases[10]. Alternatively, a diffusive transport may be assumed between mobile and immobile phases[11]. If a diffusive transport is considered between the two phases, a geometry and a size are assigned to the immobile phase. Superposition of multiple continua is required due to existence of different geometries or differing sizes of the same geometry.

A natural extension of multiple source terms is to assume the immobile phase size as a distribution function. This concept, which is one of the new developments in this field, has been successfully applied for fluid flow in porous media where the heat equation applies[5, 6].

Finally, the very far field approach is employed where the scale of flow is far greater than the scale of heterogeneities. In this approach the entire medium is treated as a single continuum representing characteristics of both mobile and immobile phases and no source term exists in the transport equation.

Except for the very far field approach, two coupled one-dimensional equations are used to represent the transport in heterogeneous systems. The dimensionless one-dimensional equation of the transport in mobile phase is given by Eq.2. Writing it in an open form, one obtains:

$$\frac{1}{P_e}\frac{\partial^2 C}{\partial x^2{}_D} - \frac{\partial C}{\partial x_D} - q_D - \frac{\partial C}{\partial t_D} = 0 \quad (9)$$

Also the nondimensionalized equation of transport in immobile phase is in the form of either:

$$\frac{1}{P_{im}}\nabla^2{}_D C_m = \frac{\partial C_m}{\partial t_D} \quad (10)$$

or:

$$K_D\frac{\partial C_m}{\partial t_D} = (C - C_m) \quad (11)$$

where

$$P_{im} = \frac{a^2 u}{D_m L} \quad (12)$$

$$K_D = \frac{u}{KL} \quad (13)$$

While Eq.10 is valid for a diffusive transfer between the two phases, Eq.11 is used when the transfer is assumed to be proportional to the average concentration difference between them. Equations 9 and 10 are coupled by using the continuity of the flux and concentration across the interface of mobile and immobile phases. Hence, the following relations holds:

$$C_R = C_m \quad on \quad \Gamma_D \quad (14)$$

$$q_D = \frac{1}{\sqrt{P_t P_{im}}}\langle\frac{\partial C_m}{\partial \eta_D}\rangle_{\Gamma_D} \quad (15)$$

where

$$P_t = \frac{(\frac{V_{fp}}{\phi A_m})^2 u}{D_m L} \quad (16)$$

Equations 9 and 11, on the other hand, are coupled through the relation:

$$q_D = \omega\frac{\partial C_m}{\partial t_D} \quad (17)$$

where ω is the ratio of the mobile phase fraction of the total pore space to the immobile phase fraction.

The presence of multiple blocks in immobile phase for the far field approach is treated as follows. Rearranging Eq.15 gives:

$$q_D = \frac{\sqrt{P_{im}}}{\sqrt{P_t}}\frac{1}{P_{im}}\langle\frac{\partial C_m}{\partial \eta_D}\rangle_{\Gamma_D} \quad (18)$$

For a finite diffusive transport medium $\sqrt{P_{im}/P_t}$ is equal to the pore volume ratio, V_{mp}/V_{fp}. Keeping this ratio constant, that is if pore volume of immobile phase increases pore volume of mobile phase increases at the same rate or vice versa, means employing a distributed approach. That means the immobile phase is uniformly distributed within the mobile phase and pore volume ratios will be equal to ω. If there are blocks of various size uniformly distributed in the field, the source term has to account for that distribution. Considering the block size is a continuous variable and the relative frequency density of blocks of size a in all blocks is $f_i(a)$, the expected total contribution is:

$$q_{DT} = \omega\int_{a_{min}}^{a_{max}}\frac{f_i(a)}{P_{im}}\langle\frac{\partial C_m}{\partial \eta_D}\rangle_{\Gamma_D} da \quad (19)$$

where

$$\int_{a_{min}}^{a_{max}} f_i(a)da = 1 \quad (20)$$

At this point it should be pointed out that all of the parameters of Eq.9 are based on the mobile phase characteristics, so that any difference between the solutions of various approaches will result only due to the source term q_D. Thus, for a comparision of solutions, observing the differences in the source term q_D will suffice.

Regardless of the approach of modelling and the type of transfer between the two phases, the source term in Eq.9 defined by either of equations 15 and 17, may be expressed as:

$$q_D = \int_0^{t_D}\frac{\partial C}{\partial \tau}\, q_{uD}(t_D - \tau)\, d\tau \quad (21)$$

where q_{uD} is the flux across the interface between the two phases for C_m being equal to unity at the interface, instead of C. Eq.21 is based on the well known convolution principle used mostly for deriving solutions of heat equation for a variable surface condition[9, 12].

Similarly, if q_D is defined by Eq.11, it may also be expressed as Eq.21. However, in this case q_{uD} will be:

$$q_{uD} = \frac{\omega}{K_D}\exp(-\frac{t}{K_D}) \tag{22}$$

Eq.21 shows that the source term is a linear function of C for all heterogeneous medium models discussed above. Consequently, the discussion on the C_R and C_F variables in the prevoius section, applies for heterogeneous medium models as well.

In summary, Eq.9 is also satisfied by C_F for all heterogeneous medium models. The corresponding dependent variable of the immobile phase transport equation namely, C_{mF} could satisfy both Eq.10 and Eq.11. As in the case of C and C_m, C_F and C_{mF} are also correlated by the same relation[13] namely:

$$C_{mF} = C_m - \frac{1}{P_e}\frac{\partial C_m}{\partial x_D} \tag{23}$$

Consequently, Eq.9 coupled with either Eq.10 or Eq.11 can be solved directly for C_F as well as for C_m.

Finally, if the source term is a nonlinear function of C_R, none of the functions derived by using linear combinations of C_R and its derivatives satisfy Eq. 9. In such a case, however, C_F does not loose its physical meaning but can only be found from the theoretical expression for C_R by using Eq. 1.

3 Classification of Solutions

If both concentration variables C_R and C_F satisfy the same equation, initial and boundary conditions determine whether the solution is in terms of C_R or C_F. In solving mathematical equations, Brigham[2] explained the proper specification of the initial and boundary conditions based on these two concentration variables. Later, Kreft and Zuber[3] provided a classification of the solutions to the convection-dispersion equation and the transformations linking the solutions.

Based on the above discussion, solutions of Eq.9 may also be classified with respect to the modes of injection and detection of tracer. However, a complete set of solutions of Eq.9, of which the instantaneous injection solutions are given in Table 1, is mostly of academic interest. The continuous injection solutions could be obtained by multiplying the instantaneous injection solutions by $1/s$. The C_{RR} and C_{RF} solutions in Table 1 seem to be presented first in this work. In addition, C_{FR} solution appeared in an earlier work[14], seem to be never used in interpretation of tracer return profiles. Nevertheless, such a classification would serve for understanding the physical meaning of C_{FF} solution, which corresponds to an injection into the fluid stream entering the system and measuring the concentration of outflowing fluid at the outlet boundary.

If, for example, one were to inject the tracer into the inflowing stream and measure the concentration within the system at an instant at the outlet boundary, one then would have to use the C_{FR} solution.

Since most of the tracer return profiles obtained from experiments are plotted in C_{FF} variable, the theoretical C_{FF} solutions of various heterogeneous medium models will be compared in the following.

4 Theoretical Return Profiles

Fig.1 shows the tracer return profiles resulting from various heterogeneities leading to different dominant transport mechanisms represented by the solutions in Table 2.

The line 1 represents the limiting case of the pure convective transport. The curves 2 and 3 represent a convective and a diffusive transport, the latter of which takes place perpendicular to the direction of flow. The difference between them results from the extent of diffusive transport medium which is infinite for line 2 and finite for line 3. Since there is no dispersion the tracer breakthrough will occur only after the convective fluid flow breakthrough. The degree of diffusive transport will determine the slope of the profile. If there are only the convective and dispersive transports mechanisms in mobile phase, the resulting figure will be similar to line 4. In this case the whole shape is affected by the dispersive transport only. The spreading of the transition zone is direcly proportional to the dispersivity of the system. Finally, the presence of all three mechanisms namely, convective, dispersive and diffusive transports yield the curves 5 and 6. The difference between these two curves also results from the extents of their diffusive transport media. The early part of the breakthrough curve will be determined mostly by the dispersive transport. The part after the convective breakthrough time will be controlled by the diffusive transport.

As mentioned earlier, the parameters are based on the mobile phase pore volume so that the solutions for all approaches could be compared. The commonly employed method of basing the parameters on the total pore volume is unable to give a way of respresenting the very near field with an infinite diffusive transport medium.

One may wish to study various alternatives in the far field approach, in addition to these fundamental models. These alternatives are defined according to the type of transfer between the two phases, geometry of the immobile phase, and discrete and continuous size distribution for multiple blocks in immobile phase.

An effective way of investigating these alternatives is a study of the behavior of block geometry functions, BGFs. The BGF may be defined as the Laplace transform of the transport rate per unit capacity of matrix block for a unit concentration at the surface of the block. The BGF is also called as effectiveness factor[15] or outflow function[16] depending on the area of study.

The Laplace transform of the source term in Eq.9 is a product of the Laplace transforms of the two terms inside the integral in Eq.21, one of which is q_{uD}. Therefore, by definition, for a finite immobile phase volume, the Laplace transform of q_{uD} will be a product of V_{mp}/V_{fp} and BGF. Hence, any difference between these alternatives will come from the difference between their BGFs.

The behavior of BGFs of principal geometries given in Table 3 were studied earlier by several authors[7, 15, 16] whose findings may be summarized as follows. Choosing their characteristic dimension as the ratio of the block volume to the surface area one may express the BGFs of basic geometries as a function of a single parameter Λ, given by:

$$\Lambda = \sqrt{sP_{im}} \qquad (24)$$

As long as volume to surface ratios of the blocks are equal BGFs of basic geometries follow one another quite closely, Fig. 2. It can also be seen that for large and small values of Λ, all curves collapses to a single curve. Therefore, one expects that the solutions would depend on the geometry only slightly.

A further point in the investigation of BGFs is the determination of the behaviors of BGFs of multiple blocks. Multiple blocks case also presents several alternatives due to the distribution type of block size. Here, however, only BGFs of uniform (rectangular) continuous size distribution will be considered. Fig.3 shows BGFs of uniform continuous size distributions for the immobile phase with respect to that of a single block having a size equal to the mean of the distribution. There are three important findings: First, for an observable variation of a multiple block BGF from that of a single block, the ratio of the minimum block size to the maximum block size, θ_{min}, must be at most 0.1. Second, the differences occur only for large Λ which corresponds to early time and large block sizes. This is the major difference between the geometrical effect and distribution effect. Finally, for θ_{min} greater than 0.01 and Λ less than 100, the difference between BGFs appears to be logarithmically proportional to θ_{min}. As a result, it seems reasonable to represent the multiple blocks with a single block of size equivalent to their mean size.

However, we need to justify that small differences in BGFs do not give rise to large differences in the complete solution. Also, we have to show that the process of inverting the Laplace transform does not enhance such differences.

The upper curves in Fig.4 shows that for the immobile phase fraction being smaller than that of the mobile phase the solutions are indeed very closely follow each other. However, as the immobile phase fraction grows close to the mobile phase fraction both geometry and presence of multiple immobile phases lead to considerable differences in solutions of these alternatives, as shown in the lower curves in Fig.4.

The higher the value of BGF the greater the diffusion rate and hence the lower the concentration values in mobile phase. This could be observed from curves of BGF and the corresponding C_{FF} solution curves.

5 Interpretation Methods

The best way of interpreting the tracer return profiles may be employing a nonlinear curve fitting method[17]. Such a method could give fast and efficient results.

Efficiency of this method depends on first using the right theoretical model and then choosing the parameters independent of each other. In addition, close initial estimates of parameters to their true values speeds convergence. Choosing the theoretical model and providing good initial estimates are considerably dependent upon the experience of the user.

Among heterogeneous medium models the far field approach solutions have the most number of parameters. These parameters are four characteristic times, t_d, t_w, t_t, and t_m corresponding respectively to four mechanisms, convection and dispersion in mobile phase, interaction between the two phases and diffusion in immobile phase. Since these parameters affect different segments of tracer return profiles they are unlikely to be correlated[18]. Therefore, the nonlinear regression method should work satisfactorily with these parameters. They relate to other parameters by:

$$t_d = \frac{L^2}{D} \qquad (25)$$

$$t_w = \frac{L}{u} \qquad (26)$$

$$t_t = \frac{(\frac{A}{\phi V_f})^2}{D_m} \qquad (27)$$

and

$$t_m = \frac{a^2}{D_m} \qquad (28)$$

If only a convective and dispersive transport is assumed, the source term in Eq.9 becomes zero and there remains only two parameters whose initial estimates may be obtained by[19]:

$$t_w \cong 2t_p - t_b \quad (29)$$

and

$$t_d = \frac{6t_w^2 t_p}{t_w^2 - t_p^2} \quad (30)$$

The model based only on a convective and diffusive transport has also two parameters, t_w and t_t, that may initially be estimated as:

$$t_w \cong t_b \quad (31)$$

$$t_t = (t_p - t_w)\frac{3}{2t_w^2} \quad (32)$$

For the far field approach solutions which include all three mechanisms of transport, the parameter t_w should be assigned an initial value which is slightly smaller than t_p. The initial estimate of the characteristic time for dispersion, t_d may be:

$$t_d \cong \left[t_d(\frac{t_w}{t_p})^2\right] \quad (33)$$

where the terms in the bracket refers to values obtained from equations 29 and 30.

The parameter t_t is again given by Eq.32. Finally, t_m should be based on the value of t_t and the tailing of tracer return profile. A pronounced tailing indicates t_t and t_m values are close. Little tailing, on the other hand, means a t_m value at least ten times smaller than that of t_t.

As an example, a model generated data set was mached by a regression procedure, Fig.5, whose generated, initially estimated and regressed parameter values are given in Table 4. Fig.5 and Table 4 together show that matching of the return profile and parameter estimation results are excellent. Even if one were to use initial estimates much different than the true values, the parameter values would still have converged. However, in such a case the regression procedure takes more iteration steps.

6 Conclusions

A distinction is necessary between the resident and flux concentrations to prevent material balance errors and incorrect interpretation of tracer return profiles resulting from employing solutions inconsistent with the actual conditions of experiments. Therefore, the classification of the solutions of classical convection dispersion model in terms of these two concentration variables is extended to include those of heterogeneous system models as well. Such a classification provides an insight into the physical meaning of solutions and help choosing the right theoretical model when interpreting an experimental tracer return profile.

Earlier works studying the influence of immobile phase geometry have shown that principal geometries yield similar block geometry function, BGF, curves. This work showed that size distribution of immobile phase also gives similar BGF curves to the BGF curve of their mean size. This particularly true for intermadiate to late times.

The questions of whether the small differences in BGFs give rise to larger differences in the complete solution or whether these differences are enhanced by the Laplace transform inversion process were also investigated. It was found that differences in BGFs yield significant differences in solutions only if the immobile phase fraction is close to or larger than that of the mobile phase.

In the interpretation of tracer return profiles use of a nonlinear regression technique is recommended. Providing close initial estimates of the parameters, which greatly speeds convergence, depends on experience of the user about the field. However, one may also use the provided formulae based on distinctive features of the experimental tracer return profiles.

7 Nomenclature

a = volume to area ratio of a matrix block
A = interface area between mobile and immobile phases
B = block geometry function
C = mobile phase concentration
C_m = immobile phase concentration
D = longitudinal dispersion coefficient
D_m = diffusion coefficient in immobile phase
f_i = relative frequency density function of immobile phase blocks
K = mass transfer coefficient
L = characteristic length of flow system
P_e = longitudinal Peclet number of mobile phase
P_{im} = Peclet number of immobile phase
P_t = transverse Peclet number of mobile phase
q = a source/sink in the system (amount of tracer generated/lost per unit volume of the mobile phase per unit time)
s = Laplace transform variable
t = time variable of the transport equations
t_b = tracer breakthrough time
t_d = characteristic time for dispersion
t_m = characteristic time for diffusion
t_t = characteristic time for interaction between two phases
t_p = peak arrival time of a tracer slug
t_w = breakthrough time of the convective front
u = flow velocity
x = space variable along the flow direction
V_{mp} = pore volume of immobile phase
V_{fp} = pore volume of mobile phase

y = space variable perpendicular to the flow direction
δ = Dirac delta function
ϕ = matrix porosity
η = space variable of diffusive transport domain
θ_{min}= the ratio of the smallest block size to largest block size
τ = time convolution variable
λ = ratio of a block to the largest block size
Λ = block geometry function parameter
∇ = gradient operator
$\mathcal{L}$ = linear Operator

subsrcipts

D = dimensionless
F = flux
mb = multiple block
R = resident
sb = single block
u = for a unit concentration at the boundary
$_{\min}$ = minimum
$_{\max}$ = maximum

superscripts

$-$ = indicates Laplace transformation
$'$ = indicates derivative

References

[1] Parker, J. C. and van Genuchten M. Th.: "Flux-Averaged and Volume-Averaged Concentrations in Continuum Approaches to Solute Transport," *Water Resour. Res.* (1984a), *20* 7, 866-872.

[2] Brigham, W. E.: "Mixing Equations in Short Laboratory Cores," *Soc. Pet. Eng. J.*, (1974), *14*, 91-99.

[3] Kreft, A. and Zuber, A.: "On the Physical Meaning of the Dispersion Equation and its Solutions for Different Initial and Boundary Conditions," *Chem. Eng. Sci.* 33, (1978), *33,* 1471-1480.

[4] Bear, J. and Berkowitz, B: " Groundwater Flow and Pollution in Fractured Aquifers," *Developments in Hydraulic Engineering, Vol. 4* , P. Novak (Editor), Elsevier, London, (1987), 175-235.

[5] Cinco-Ley, H., et. al. : " The Pressure Transient Behavior For Naturally Fractured Reservoirs with Multiple Block Size," *SPE 14168,* presented at the 60th Fall Technical Conference held in, Las Vegas, NV,Sept., (1985).

[6] Katsunori, F. : " Rate Decline Analysis for Naturally Fractured Reservoirs," Masters Report, Stanford University, (1989).

[7] Barker, J. A. : "Block Geometry Functions Characterizing Transport in Densely Fissured Media," *J. Hydrol.,* (1985), *7,* 263-279.

[8] Clark, R. T.: "A Review of Some Mathematical Models Used in Hydrology with Observations on Their Calibration and Use," *J. Hydr.*, (1973), *19,* 1-20.

[9] Carslaw, H. S. and Jeager, J. C.: *Conduction of Heat in Solids,* Clarendon Press, Oxford, (1986), 75-77.

[10] Coats, K. H. and Smith, B. D. : "Dead-end Pore Volume and Dispersion in Porous Media," *Soc. Pet. Eng. J., Trans. AIME, 231,* (March 1964), 73-84.

[11] Passioura, J. B.: "Hydrodynamic Dispersion in Aggregated Media: I. Theory," *Soil Sci.,* (1971a), *3,* 6, 339-344.

[12] de Swaan, O. A.: " Analytical Solution for Determining Naturally Fractured Reservoir Properties by Well Testing," *Soc. Pet. Eng. J.,* (June, 1976)

[13] Baker,L. E.: "Effects of Dispersion and Dead-End Pore Volume in Miscible Flooding," *Soc. Pet. Eng. J.,* (June 1977), 219-227.

[14] Correa, A. C., Pande, K. K., Ramey, H. J. Jr. and Brigham, W. E.: "Prediction and Interpretation of Miscible Displacement Using a Transverse matrix Dispersion Model," *SPE 16704,* (Sep. 1987).

[15] Aris, H. : " On the Shape Factors for Irregular Particles-I,"*Chem. Eng. Sci., vol. 6* (1957), 262-268.

[16] de Swaan, O. A.: " Influence of Shape and Skin of Matrix-Blocks on Pressure Transients in Naturally Fractured Reservoirs," *SPE 15637,* Presented at the 61st Technical Conference held in, New Orleans, LA, (Oct.,1986).

[17] Rosa, A. J. and Horne, R. N. : " Automated Type-Curve Matching in Well Test Analysis Using Laplace Space Determination of Parameter Gradients," *SPE 12131,* presented at the 1983 SPE Annual Meeting held in, San Fransisco, CA, (Oct.,1983).

[18] De Smedt, F., Wierenga, P. J. and Van der Beken, A.: *Theoretical and Experimental Study of Solute Movement Through Porous Media with Mobile and Immobile Water,* Vrije Universtait Brussel, Brussel, (1981).

[19] Bullivant, D. P.: "Tracer Testing of Geothermal Reservoirs," Ph.D. Thesis, Department of Theoretical and Applied Mechanics, School of Engineering, University of Auckland, Auckland, New Zealand, (1988).

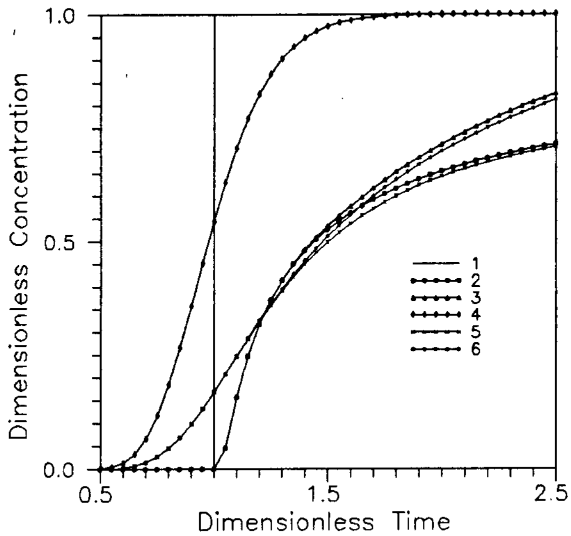

Figure 1: Theoretical Tracer Return Profiles of Fundamental Models

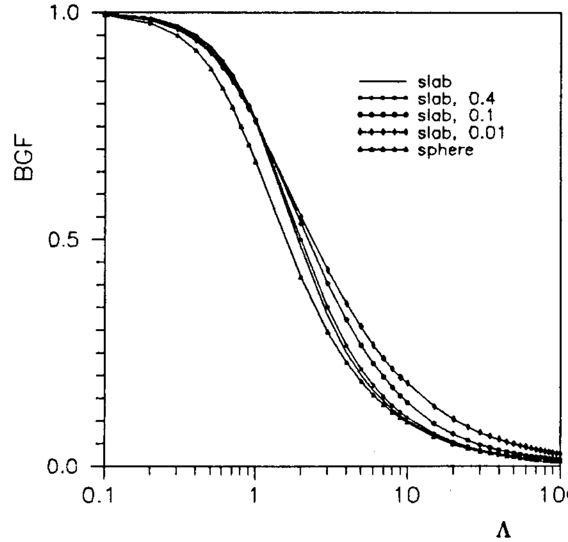

Figure 3: BGFs for Uniform Frequency Distribution

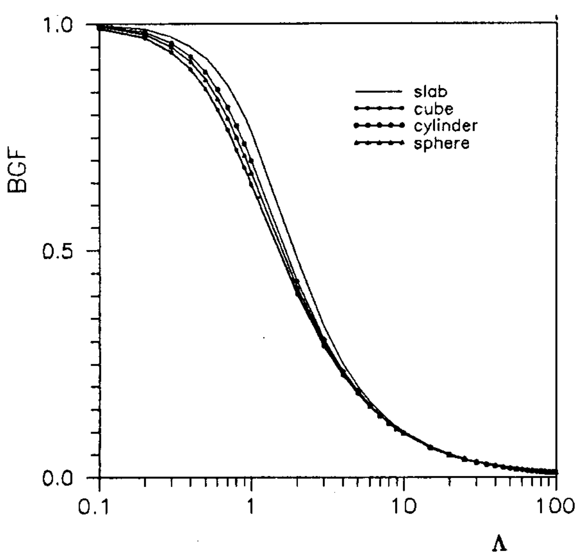

Figure 2: BGFs for Principal Geometries, [after Barker 1985]

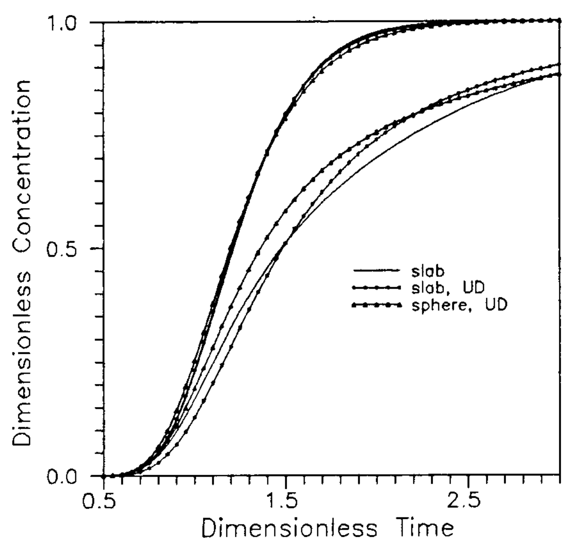

Figure 4: Tracer Return Profiles for Various Immobile Phase Geometries and Distributions

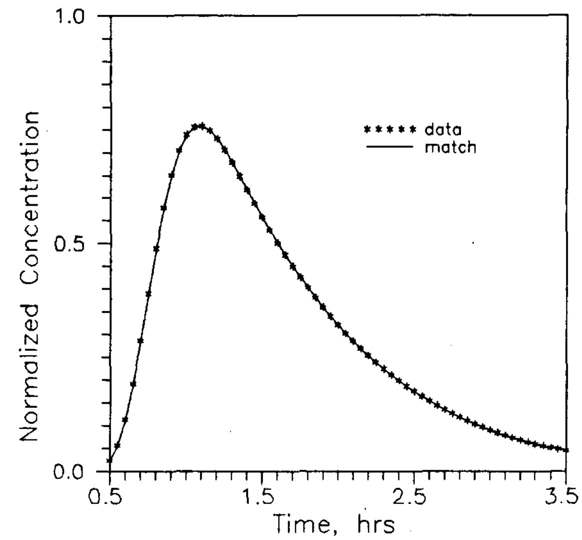

Figure 5: Matching a Data Set by Nonlinear Regression Method

IC & BC	Solution
$C(x_D,0)=\delta(x_D),\ C_m(x_D,y_D,0)=0$ $\lim_{x_D\to-\infty} C(x_D,t_D)=0$ $\lim_{x_D\to\infty} C(x_D,t_D)=0$ $C(x_D,t_D)=C_m(x_D,0,t_D)$ 2^{nd} BC for C_m	$\overline{C}_{RR}=\frac{2}{\gamma(s)}\exp\left[(1-\gamma(s))\frac{P_e\lvert x_D\rvert}{2}\right]$
$C(x_D,0)=(\delta(x_D)-\frac{1}{P_e}\delta'(x_D))$ $C_m(x_D,y_D,0)=0$ $\lim_{x_D\to\mp\infty} C(x_D,t_D)=0$ $C(x_D,t_D)=C_m(x_D,0,t_D)$ 2^{nd} BC for C_m	$\overline{C}_{RF}=\frac{1+\gamma(s)}{2\gamma(s)}\exp\left[(1-\gamma(s))\frac{P_e x_D}{2}\right]$
$C(x_D,0)=C_m(x_D,y_D,0)=0$ $[C-\frac{1}{P_e}\frac{\partial C}{\partial x_D}]_{x_D=0}=\delta(t_D)$ $\lim_{x_D\to\infty} C(x_D,t_D)=0$ $C(x_D,t_D)=C_m(x_D,0,t_D)$ 2^{nd} BC for C_m	$\overline{C}_{FR}=\frac{2}{1+\gamma(s)}\exp\left[(1-\gamma(s))\frac{P_e x_D}{2}\right]$
$C(x_D,0)=C_m(x_D,y_D,0)=0$ $C(0,t_D)=\delta(t_D)$ $\lim_{x_D\to\infty} C(x_D,t_D)=0$ $C(x_D,t_D)=C_m(x_D,0,t_D)$ 2^{nd} BC for C_m	$\overline{C}_{FF}=\exp\left[(1-\gamma(s))\frac{P_e x_D}{2}\right]$

where $\gamma(s)=\sqrt{1+\frac{4s}{P_e}(1-\overline{q}_{uD}(s))}$, and

2^{nd} BC of C_m and hence $\overline{q}_{uD}(s)$ depends on the modelling approach

Table 1: Instantaneous injection solutions of heterogeneous medium models

Mechanisms	Solution
Convection & Diffusion	$C_{D_{sf}} = \frac{1}{s}\exp\left(-s-\sqrt{s/P_t}\right)$
	$C_{D_{pf}} = \frac{1}{s}\exp\left(-s-\sqrt{s/P_t}\, tanh\sqrt{sP_{im}}\right)$
Convection & Dispersion	$C_D = \frac{1}{s}\exp\left[\left(1-\sqrt{1+4s/P_e}\right)P_e/2\right]$
Convection Dispersion & Diffusion	$C_{D_{sf}} = \frac{1}{s}\exp\left[\left(1-\sqrt{1+4(s+\sqrt{s/P_t})/P_e}\right)P_e/2\right]$
	$C_{D_{pf}} = \frac{1}{s}\exp\left[\left(1-\sqrt{1+4(s+\sqrt{s/P_t}\, tanh\sqrt{sP_{im}})/P_e}\right)P_e/2\right]$
	$C_{D_{sb}} = \frac{1}{s}\exp\left[\left(1-\sqrt{1+4s(1+\omega B_{sb}(\Lambda))/P_e}\right)P_e/2\right]$
	$C_{D_{mb}} = \frac{1}{s}\exp\left[\left(1-\sqrt{1+4s(1+\omega B_{mb}(\Lambda))/P_e}\right)P_e/2\right]$

Table 2: Solutions of Fundamental Transport Models

	Geometry	Block Geometry Function, $B(\Lambda)$
Single Block Size	Slab	$tanh(\Lambda)/\Lambda$
	clinder	$I_1(2\Lambda)/(\Lambda I_0(2\Lambda))$
	sphere	$coth(3\Lambda)/\Lambda - 1/(3\Lambda^2)$
	cube	$512/\pi^6 \sum_{i=1}^{\infty}\sum_{j=1}^{\infty}\sum_{k=1}^{\infty}\left[\alpha_{ijk}/(\alpha_{ijk}+\Lambda^2)\right]/(ijk)^2$ $where\ \ \alpha_{ijk} = (\pi/6)^2(i^2+j^2+k^2)\ \ i,j,k\ \ odd\ \ integers$
Multiple Block Size	slab, uniform distribution	$1/(1-\lambda_{min})\int_{\lambda_{min}}^{1} tanh(\Lambda_{max}\lambda)/(\Lambda_{max}\lambda)\, d\lambda$ $where\ \ \lambda = a/a_{max}\ \ and\ \ \Lambda_{max} = \sqrt{s(P_{im})_{max}}$

Table 3: Block Geometry Functions for Principal Geometries [after Aris,1957 and Barker 1985

parameter	generator value	initial estimate	regressed value
t_d	30.0	26.5	30.0
t_w	1.0	0.9	1.0
t_m	2.5	2.08	2.5
t_{im}	1.0	1.5	1.0

Table 4: The Parameter Values of Regression Shown in Fig. 5.